Adsorption Mechanism of Carbon Dioxide in Faujasites: Grand Canonical Monte Carlo Simulations and Microcalorimetry Measurements

G. Maurin,*,†,‡ P. L. Llewellyn,† and R. G. Bell§

Laboratoire MADIREL, UMR CNRS 6121, Université de Provence, Centre St Jérôme, Av. Escadrille Normandie Niemen, 13397 Marseille Cedex 20, France, Laboratoire LPMC, UMR CNRS 5617, Université Montpellier II, Pl. E. Bataillon, 34095 Montpellier Cedex 05, France, and The Davy Faraday Research Laboratory, Royal Institution of Great Britain, London W1S 4BS, U.K.

Received: May 24, 2005; In Final Form: June 22, 2005

Molecular simulations have been coupled with adsorption microcalorimetry measurements in order to understand more deeply the interactions between carbon dioxide and various types of faujasite surfaces. The modeling studies, based on newly derived interatomic potentials for describing the interactions within the whole system, provide isotherms and evolutions of the differential enthalpy of adsorption as a function of coverage for DAY, NaY, and NaLSX which are in very good accordance with those obtained experimentally. The microscopic mechanism of CO_2 adsorption was carefully analyzed, with different behaviors proposed, depending on the energetic characteristics of each faujasite surface, which are consistent with the trends observed for the differential enthalpies of adsorption.

1. Introduction

One of the technological and environmental problems that society faces today is the environmentally friendly and economically favorable separation, capture, and storage of gases. This is particularly the case for gases such as carbon dioxide and hydrogen that will be increasingly important in the future world economy.[1] The excessive emission of carbon dioxide into the atmosphere not only leads to the global warming effect[2] but also may be at the origin of health problems.[3] Indeed, the increase in carbon dioxide emission leads plants and molds to increase pollen and spore production which is argued as one of the causes of the rises in asthma cases, especially among children.[3] Furthermore, hydrogen is commonly produced from "reformed" natural gas creating both carbon monoxide and dioxide as byproducts which must be removed to generate high-purity hydrogen for fuel cells.[4] In this way, selective separation of carbon oxides is a key point for the development of the hydrogen economy. It thus appears that efficient carbon dioxide separation and storage with a minimal environmental impact and low costs are of great importance. The currently used amine-based systems for carbon dioxide removal have several disadvantages, such as additional processing and corrosion control.[5] Such problems can be overcome by using a pressure swing adsorption (PSA)-based system.[6] The PSA system is known to be one of the most efficient and economical processes to recover carbon dioxide in flue streams from power plants and incinerators. The selection of the most suitable adsorbent for such adsorption-based separation processes is then a crucial point as its efficiency strongly depends on the adsorbent's performance. Among the potential adsorbent nanoporous candidates (i.e., activated carbons, metal organic frameworks, clays, silicas, etc.), zeolites, which are well-ordered microporous systems,[7] are very promising materials for selective adsorption and separation of carbon dioxide.[8,9] They are of great interest because their properties influencing the adsorption performance such as pore size and architecture or chemical composition, for instance Si/Al ratio and the nature of extraframework cations, can be varied systematically.[10,11] In addition to their environmentally friendly character and their strong affinity for carbon dioxide,[8,9] zeolite systems have been revealed to be stable under vacuum up to high temperatures which make them ideal for PSA-type applications. It has been previously reported that narrow pore size zeolites such as Na-4A[8] and CaA[12] are the most suitable for this purpose. It was also pointed out that zeolite 13X can be used as a carbon dioxide storage medium at low temperatures and pressures; its adsorption capacity being preferred to that of activated carbon.[13] More recently, a study based on an exhaustive zeolite adsorbent screening reported that the most promising adsorbents for carbon dioxide sequestration are characterized by a low Si/Al ratio and contain extraframework cations that give strong electrostatic interactions with carbon dioxide.[14] For given operating conditions corresponding to low-pressure carbon dioxide feed and regeneration, 13X and NaY are claimed to be the most suitable adsorbents. Furthermore, zeolite membranes which are able to sustain more severe conditions such as high temperature and pressure and chemical corrosion, compared with polymer membranes, are also attractive for carbon dioxide capture and separation.[15] It has been recently shown that high silica ZSM-5 membranes combining suitable pore size and shape selectivity provide high performance for carbon dioxide sequestration from methane-reforming processes.[16]

Furthermore, zeolite membranes combined with noble metals can also successfully be used as catalysts[17,18] for reforming undesirable carbon dioxide into synthesis gas which can be further converted via various chemical reactions such as Fischer Tropsch synthesis[19] into fuels. This latter process provides an alternative route for application in the storage of renewable

* To whom correspondence should be addressed. E-mail: gmaurin@lpmc.univ-montp2.fr. Tel: +33 4 67 14 33 07. Fax: +33 4 67 14 42 90. Present address: Laboratoire LPMC UMR CNRS 5617, Université Montpellier II, Pl. E. Bataillon, 34095 Montpellier cedex 05.

† Université de Provence.

‡ Université Montpellier II.

§ Royal Institution of Great Britain.

10.1021/jp052716s CCC: $30.25
Published on Web 07/30/2005

energy sources.[20] Such an ambitious application also requires an initial deep understanding of the interactions between carbon dioxide and the zeolite surface. Furthermore, it has to be emphasized that the number of investigations related to carbon dioxide adsorption in zeolite systems at high pressure is limited[21−23] although this is of crucial interest for gas storage technology.[24]

Zeolite adsorbent properties with respect to carbon dioxide are commonly evaluated by determining the adsorption isotherms via gravimetric and volumetric measurements, Henry's constants, and enthalpies of adsorption.[14] These latter thermodynamic data reported in the literature are mainly estimated by using isosteric methods.[25−28] The enthalpies of adsorption, thus calculated by differentiation of the Clausius−Clapeyron equation, are very sensitive to errors in the adsorption isotherms. By contrast with this technique, which suffers from the inaccuracy associated with differentiation, few attempts have been made using microcalorimetry[29−31] which offers the great opportunity directly to access the differential enthalpy of adsorption with a high accuracy. In this paper, we selected various types of energetic faujasite surfaces by modifying the Si/Al ratio; the purely siliceous form DAY is compared to NaLSX and NaY which are characterized by different Si/Al ratios. The characterization of adsorbate/adsorbent interactions is performed by combining adsorption microcalorimetry experiments up to 35 bar and molecular simulations. From an experimental standpoint, adsorption microcalorimetry is a powerful technique which has been extensively applied to characterize both adsorbent surfaces and various adsorption phenomena occurring in nanoporous materials.[32] Such measurements using polar and nonpolar probes have been able to characterize the adsorption sites in various energetically homogeneous and heterogeneous zeolite systems.[33,34] Here, the differential enthalpies of adsorption at 300 K over a large domain of pressure [0, 35 bar] are reported as well as the isotherms of adsorption for carbon dioxide in the various forms of faujasites. From a theoretical point of view, grand canonical Monte Carlo (GCMC) simulations are the most suitable for establishing a correlation between the microscopic behavior of the zeolite/adsorbate system and the equilibrium thermodynamic properties.[10,35] They depend on reliable interatomic potentials needed to reproduce as accurately as possible the interactions between the adsorbate and the zeolite framework and between the adsorbate molecules themselves which can be derived either by ab initio calculations[36] or by a semiempirical approach.[10] Only a limited number of theoretical studies have been reported concerning the adsorption and diffusion of carbon dioxide in zeolite systems:[15,21,22,37,38] (i) The diffusion of CO_2 inside the pores of ion-exchanged X-type zeolites and in zeolite membrane was investigated by combining molecular dynamics simulations and commercial force fields.[15,37] (ii) Grand canonical Monte Carlo simulations were performed on Na-4A[21] and Na−ZSM-5[22] systems based on interatomic potentials with parameters determined by fitting the experimental data. As the literature did not provide accurate and robust force fields, our first step consisted of deriving a self-consistent set of potential parameters by using ab initio clusters calculations able to describe the interactions between carbon dioxide and the cations containing zeolite and between the adsorbate molecules themselves as well as being simple enough to be transferable between different zeolite systems. From these new interatomic potentials, the adsorption properties of the various faujasite systems evaluated by GCMC simulations are reported including both the differential enthalpies and the isotherms of adsorption up to high pressure. These simulated data are then compared and contrasted with those measured experimentally in order to test the validity of the derived force fields. To the authors' knowledge, it is the first time that such a nice agreement between experiment and simulation is obtained for the adsorption of carbon dioxide in zeolite systems over a wide range of pressure. From these successful simulations, the next step consisted of proposing the microcospic mechanisms for CO_2 adsorption in each of the faujasite systems which are consistent with the evolution of the differential enthalpy of adsorption as a function of the coverage.

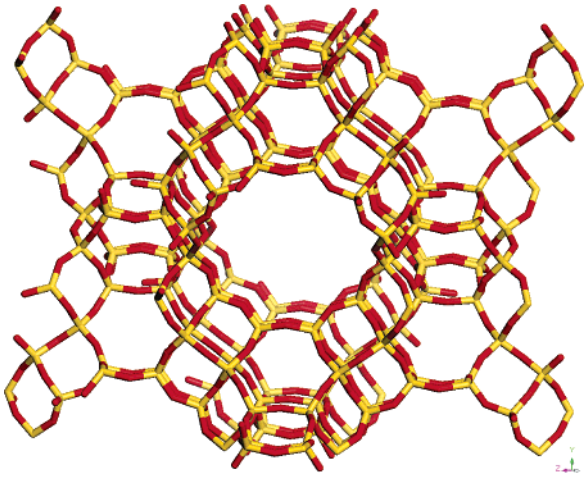

Figure 1. Representation of the faujasite framework showing supercages and sodalite cages.

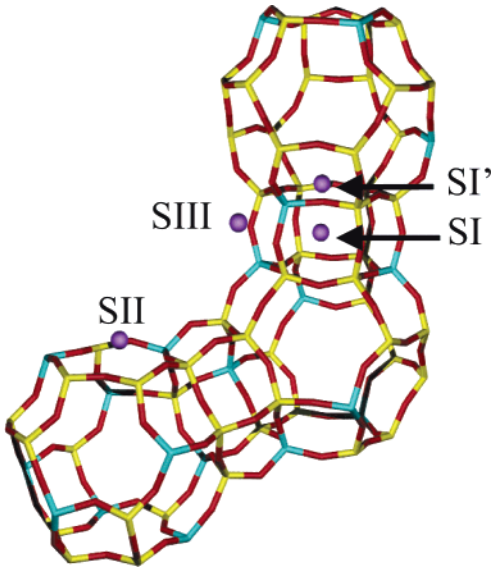

Figure 2. Description of the main crystallographic sites (I, I′, II, and III) for the extraframework cations.

2. Experimental Section

Materials and Characterization. The structure of the faujasite system used in this investigation consists of large cavities (supercages) which have roughly spherical symmetry and diameter of around 12.5 Å with a window size of 7.4 Å. Each cavity is connected to four others in a tetrahedral arrangement. The structure also contains sodalite cage units linked together by six double rings[7](Figure 1). The monovalent extraframework cations preferentially occupy different crystallographic sites named I, I′, II, and III[39] as depicted in Figure 2.

The three samples (DAY, NaY, and NaLSX) kindly supplied by Air Liquide (France) were carefully characterized, and their

chemical compositions were determined by using electron dispersive spectroscopy (EDS). The dealuminated Y zeolite (DAY) used in this investigation corresponds to the highly siliceous form of faujasite. This sample was obtained by dealumination treatment via a steaming process, and the chemical analysis provided the following composition $Na_{1.9}Al_{1.9}Si_{190.1}O_{384}$ corresponding to a Si/Al ratio = 100. NaLSX and NaY are characterized by Si/Al ratios equal to 1 and 2.4, respectively. Powder X-ray diffraction revealed the samples to be highly crystalline, and the diffractograms thus obtained showed all the characteristic peaks closely matching those reported in the literature.[7] Furthermore, the morphology and the texture of NaLSX and NaY examined by scanning electron microscopy (SEM) are typical of those previously reported elsewhere, showing crystallites of 2−3 μm size with a nearly spherical shape.[40] By contrast, the texture of the surface for DAY is different from those observed for both NaY and NaLSX which means that possible textural defects have been created by the dealumination process.

High purity (99.995%) carbon dioxide was kindly supplied by Air Liquide (France).

Microcalorimetry Measurements. Prior to each adsorption experiment, the sample was outgassed using sample controlled thermal analysis, SCTA.[41] The conditions maintain a constant residual vacuum pressure of 0.02 mbar up to a final temperature of 720 K which was kept until the residual pressure dropped to below 5×10^{-3} mbar. The adsorption at 300 K up to 35 bar was carried out by means of a Tian−Calvet-type isothermal microcalorimeter coupled with a manometric device built *in house*. This microcalorimeter consists of two thermopiles mounted in electrical opposition. Each thermopile is comprised of around 500 chromel−alumel thermocouples.[33] This complete apparatus allowed us to obtain both the isotherms and the pseudodifferential enthalpies of adsorption as a function of the coverage in each faujasite system. It has to be mentioned that all the reported experimental data will correspond to the absolute adsorption obtained from the correction of the primary excess values as follows for ideal gases (equation 1)

$$n^{a} = n^{\sigma} + \frac{pV^{zeo}}{RT} \tag{1}$$

where n^{a} and n^{σ} are the absolute and excess amount adsorbed, respectively, and v^{zeo} is the micropore volume of the various samples estimated from a *t*-plot of nitrogen physisorption measurement at 77 K. However for such studies at ambient temperature and high pressure, an appropriate expression for gas nonideality was included using the Redlich−Kwong equation of state.[42] Finally, a point-by-point adsorptive dosing procedure detailed elsewhere[43] was used to evaluate pseudodifferential enthalpy of adsorption noted $\Delta_{ads}h$ with a maximum bar error of 0.6% in the whole range of pressure.

3. Computational Methodology

The crystal structure of the various faujasite systems was modeled as follows. The purely siliceous faujasite $Si_{192}O_{384}$ with a cubic unit cell and lattice parameter of 24.8 Å[44] was considered to model the DAY zeolite. This assumption is a reasonable first approximation because the DAY sample has a Si/Al ratio of 100 which corresponds only to 1.9 residual Na^{+} per unit cell, and no experimental data are available in the literature about the location of these extraframework cations. The chemical composition $Si_{192-x}Al_xNa_xO_{384}$ was considered with $x = 92$ and $x = 56$ in order to mimic the Si/Al ratio equal to 1 and 2.4 for NaLSX and NaY, respectively. The zeolite framework was built in accordance with Löwenstein's Al−O−Al avoidance rule.[45] The second step consisted of modeling the distribution of the extraframework cations among the different crystallographic sites. For the NaLSX zeolite, the distribution defined by Seff et al.[46] was selected corresponding to 32 Na^{+} in site I′ located in the sodalite cage in front of the 6-ring window connected to the hexagonal prism and 32 Na^{+} in site II, 28 in site III′, 12-ring and 4-ring windows of the supercages, respectively (Figure 2). In this latter case, 4 positions from the initial 32 in site III′ were randomly removed, and the structure was energy minimized before the GCMC simulations. The distributions of the extraframework cations for NaY were defined as follows with 6 cations in site I located in the center of the hexagonal prism connecting two sodalite cages, 18 in site I′, and 32 in site II in close agreement with those determined experimentally by Fitch et al.[44]

TABLE 1: Pair Potential Parameters Derived from ab Initio Calculations for Both CO_2/CO_2 and CO_2/Zeolite Adsorbent Used in the GCMC Simulations

interacting pairs	ϵ (eV)	σ (Å)	interacting pairs	ϵ (eV)	σ (Å)
O−O	0.00659	3.36	O−O_z	0.00601	3.48
C−C	0.00402	3.83	C−Na	0.00759	3.35
O−C	0.00158	3.31	O−Na	0.00270	2.95
C−O_z	0.00363	3.90			

The total energy of the zeolite framework and adsorbed molecules (E) is expressed as the sum of the interaction energies between the adsorbate and the zeolite (E_{AZ}) and that between the adsorbates (E_{AA})

$$E = E_{AZ} + E_{AA} \tag{2}$$

E_{AZ} and E_{AA} are both written as sums of pairwise additive potentials of the form

$$e_{ij} = 4\epsilon_{ij}\left[\left(\frac{\sigma_{ij}}{r_{ij}}\right)^{12} - \left(\frac{\sigma_{ij}}{r_{ij}}\right)^{6}\right] + \frac{q_i q_j}{r_{ij}} \tag{3}$$

where the first term is the repulsion−dispersion Lennard-Jones potential (LJ) with ϵ_{ij},σ_{ij} corresponding to the parameter sets for each interacting pairs, and the second term is the Coulombic contribution between point charges q_i,q_j separated by a distance r_{ij}.

The faujasite system is assumed to be semi-ionic with atoms carrying as previously reported[10] the following partial charges (in electron units): Si (+2.4), Al (+1.7), O_z (−1.2), and Na (+0.7). The polarizabilities of silicon and aluminum atoms which are much lower than those of the oxygen atoms suggest that the repulsion dispersion contribution of the zeolite can be assigned only to oxygens of the framework (O_z) and extraframework cations (Na^{+}). For carbon dioxide, we used an atomic point charge model in which the charges (in electron units) assigned to the carbon C (+0.72) and the oxygen O (−0.36) atoms were obtained by ab initio calculations.[47] These charges were scaled from the Mulliken charges in order to reproduce both the heats of adsorption in silicate and the solid CO_2 structure realistically.

The LJ parameters for modeling both adsorbate−adsorbent and adsorbate−adsorbate repulsion−dispersion interactions were obtained by fitting the potential energy surfaces derived by ab initio cluster calculations using Cadpac. These calculations are reported in more detail elsewhere.[47] Here, we report the LJ parameters in Table 1 required to calculate the total energy (E).

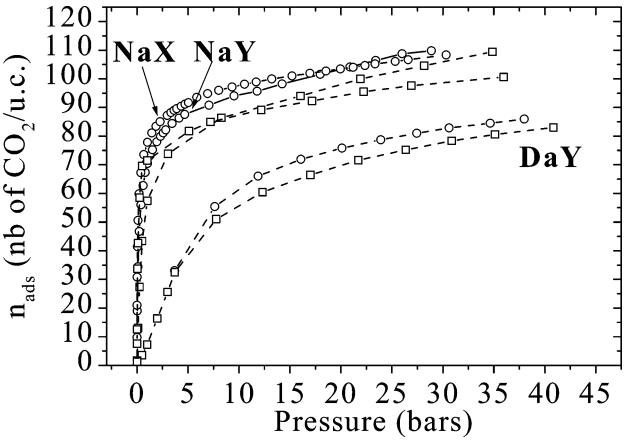

Figure 3. Absolute isotherms for carbon dioxide adsorption on DAY, NaY, and NaLSX at 300 K in the range of pressure 0−35 bar: (□) simulation, (○) experiment.

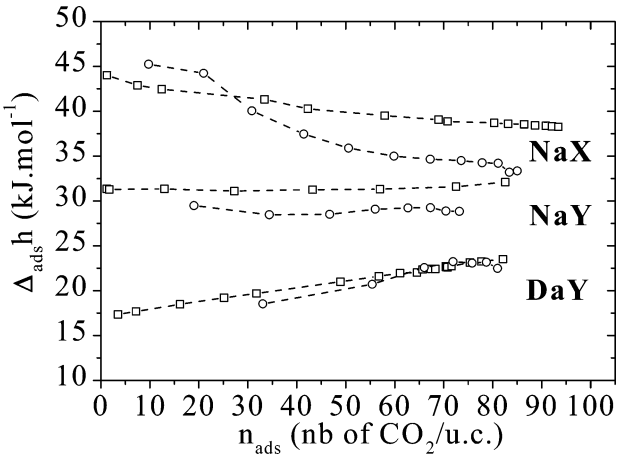

Figure 4. Evolution of the differential enthalpies of adsorption ($\Delta_{ads}\dot{h}$) as a function of the coverage for DAY, NaY, and NaLSX at 300 K: (□) simulation, (○) experiment.

Absolute adsorption isotherms were then computed using a GCMC calculation algorithm which allows displacements (translations and rotations), creations, and destructions as implemented in the *Sorption* module of the Cerius2 software suite. These simulations consisted of evaluating the average number of adsorbate molecules whose chemical potential equals those of the bulk phase for a given pressure and temperature. All these simulations were performed at 300 K using one unit cell of each faujasite system typically with 4×10^6 to 5×10^6 Monte Carlo (MC) steps. The evolution of the total energy over the MC steps was plotted in order to control the equilibrium conditions. The zeolite structure was assumed to be rigid during the sorption process. This assumption is not so drastic as the flexibility of the lattice more significantly influences the diffusion properties.[48]

The Ewald summation was used for calculating electrostatic interactions, and the short-range interactions were calculated with a cutoff distance of 12 Å. Furthermore, as its kinetic diameter (3.3 Å) is much greater than those of the six-ring opening windows of the sodalite cages (2.2 Å), carbon dioxide cannot access the sodalite cages and dummy atoms with appropriate van der Waals radiii were placed in these cages. This was done in order to avoid any introduction of adsorbates in this space, thus leading to accessibility for gas only in the supercages. The calculation of the differential enthalpies of adsorption at zero coverage $\Delta_{ads}\dot{h}_{\theta=0}$ at 300 K was performed through the fluctuations over the number of particles in the system and from fluctuations of the internal energy U[49] by considering very low pressure and switching off the adsorbate−adsorbate interactions

$$\Delta_{ads}\dot{h} = RT - \frac{\langle UN\rangle - \langle U\rangle\langle N\rangle}{\langle N^2\rangle - \langle\langle N\rangle\rangle^2} \qquad (4)$$

4. Results and Discussions

Figure 3 reports the absolute isotherms for carbon dioxide adsorption on DAY, NaY, and NaLSX obtained both experimentally and theoretically at 300 K. It has to be mentioned that this adsorbate deviates from ideal gas behavior in the whole range of pressure, and consequently, the experimental and simulated data were corrected to take into account this nonideal state. We observe that the simulated absolute isotherms reproduce well the experiments for DAY and only slightly underestimate the loading at higher pressure for NaY and NaLSX. The adsorption capacities for both NaY and NaLSX at high pressure are quite similar as was already pointed out by Choudhary et al.[26] at lower pressure and are close to the saturation loading previously extrapolated for NaX.[28] This result emphasizes that the cation density within the supercage does not strongly influence the CO_2 capacity. The CO_2 affinities for these adsorbents, which can be estimated from the slope of the isotherms in the initial low domain of pressure, increase in the order DAY, NaY, and NaLSX. A more pronounced affinity for NaLSX in the case of quadrupolar gases has been already attributed to the presence of more accessible extraframework cations located in site III.[50] Furthermore, this trend is consistent with those observed for the differential enthalpies of adsorption at zero coverage, which can be estimated from Figure 4 which reports the experimental evolutions of the differential enthalpies of adsorption as a function of the coverage for the three different faujasite forms. The interest in measuring the evolution of such thermodynamic data relies on the characterization of the adsorbent surface with respect to a given adsorbate. It is well established that a decrease in the differential enthalpy of adsorption as a function of the gas loading can be ascribed to a heterogeneous adsorbent and that a flat profile corresponds to a balance between increasing adsorbate−adsorbate interactions and an energetic heterogeneity of the adsorbent surface. By contrast, an increase in the differential enthalpy of adsorption reveals a relatively homogeneous environment for adsorbate/adsorbent interactions. The calorimetric evolutions of the differential enthalpies of adsorption for DAY, NaY, and NaY reported in Figure 4 highlight these different types of interaction behaviors with decreasing (NaLSX), constant (NaY), or increasing (DAY) values of the differential enthalpy of adsorption as a function of the loading. The simulations were performed to deeper understand these adsorption phenomena at the microscopic scale. As can be observed in this figure, a very good agreement both in the profile and in the values is obtained between experiment and simulation for each investigated system.

The differential enthalpy of adsorption in DAY is about 17.5 kJ mol^{-1} at the initial stage of loading, and it increases with surface coverage. Similar profiles have already been obtained for other siliceous zeolites such as silicalite.[27,29,51] We observed that the carbon dioxide molecules are more-or-less homogeneously distributed within the supercage with some preferential adsorption sites close to the region of the 12-ring window. Sites II and III′ in the 6- and 4-ring windows are depicted in Figure 5. Our simulation also showed by means of the calculation of the radial distribution functions that the average distance between the oxygen of the framework and the oxygen of the

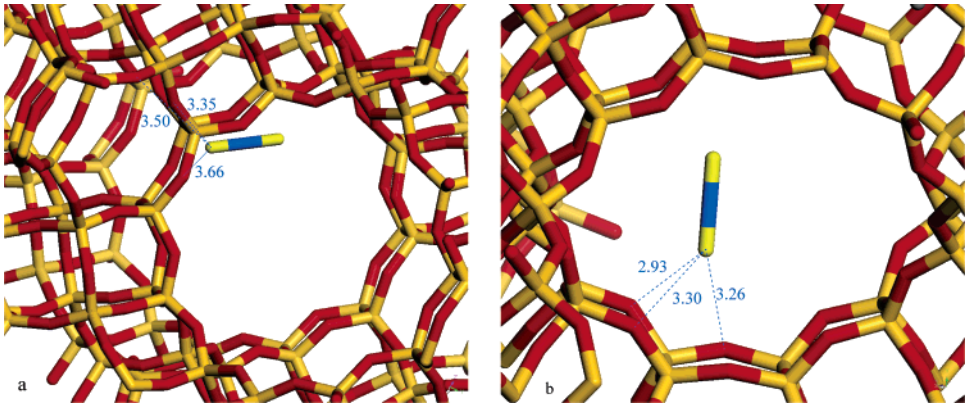

Figure 5. Representation of the preferential adsorption sites for CO_2 in DAY within the supercage close to six-ring (a) and four-ring (b) windows with the corresponding distances in angstroms.

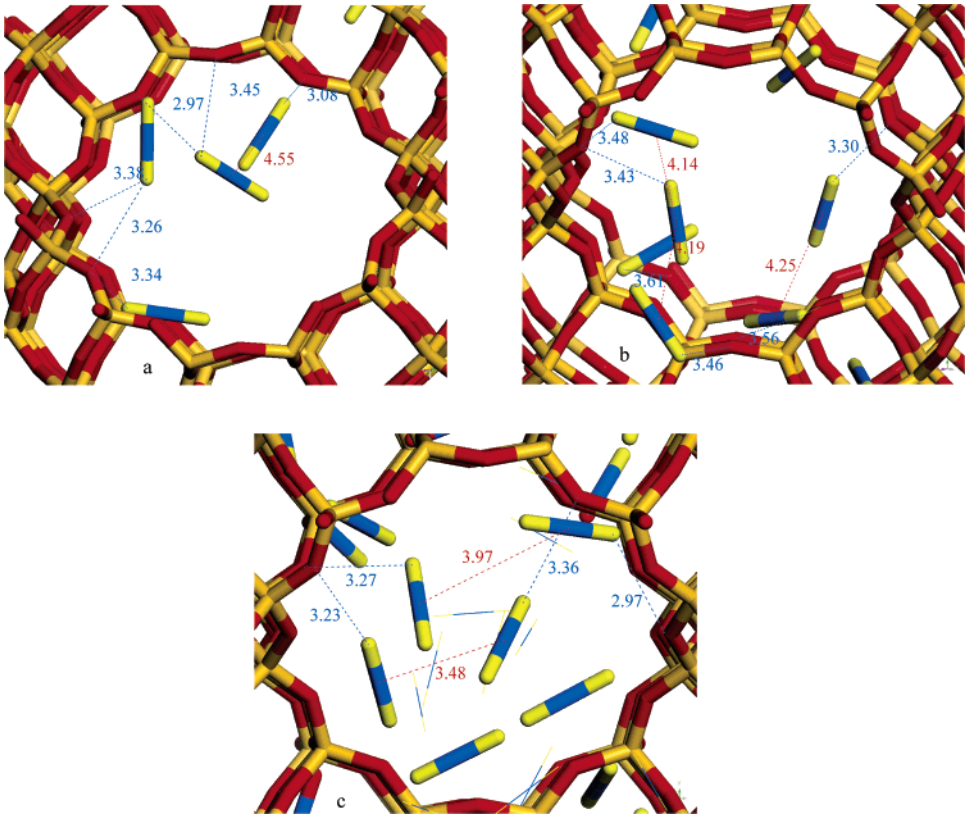

Figure 6. Typical arrangements of the CO_2 molecules in DAY for low ((a) 2 bar), intermediate ((b) 5 bar), and high ((c) 30 bar) loading. The indicated distances C−C (Å) are shorter for high loading whereas the distances O_z−O (Å) remain almost unchanged.

carbon dioxide remains almost unchanged when the loading increases, whereas those between the carbon dioxide molecules, *d*(C−C), become significantly shorter, leading to an increase of the adsorbate−adsorbate interaction energy.[52] An illustration is provided in Figure 6 with three typical arrangements of CO_2 within the supercage corresponding to low, intermediate, and high loading. Indeed, carbon dioxide probes DAY as a homogeneous energetic surface with an almost constant CO_2/adsorbent interaction energy and a CO_2/CO_2 contribution increase with loading, thus leading to an increase in the differential enthalpy of adsorption with coverage as reported in Figure 4.

An almost flat enthalpy profile is obtained for NaY with values centered around 29.5 and 31 kJ mol^{-1} for the experiment and simulation, respectively (Figure 4). The evolution is similar to those already reported in the same domain of pressure[23] with values more in accordance with those obtained by Burevski et al.[53] Our simulation indicated a single preferential adsorption site for CO_2 interacting with Na^+ located in site II. This observation is in accordance with IR spectroscopy data reported in the literature, which have measured characteristic stretching vibrations of CO_2 in a series of cation-exchanged Y zeolites.[54] The picture in Figure 7a corresponding to a low loading state, clearly shows that carbon dioxide molecules interact with Na^+ (site II) with a linear geometry ($Na^+\cdots O{=}C{=}O$). This observation has been already pointed out in other zeolite systems.[55,56] As the loading increases (parts b and c of Figure 7), the adsorbate is still interacting with Na^+ (site II) which is more and more solvated by the surrounding CO_2 molecules, and if we define ϕ as the angle between the molecular axis of carbon dioxide and the direction defined from its center of mass to Na^+, then we can observe that ϕ strongly deviates from its value of 0°, that is, end-on coordination, at the initial stage of loading. Indeed, the CO_2/NaY interaction energy slightly decreases due

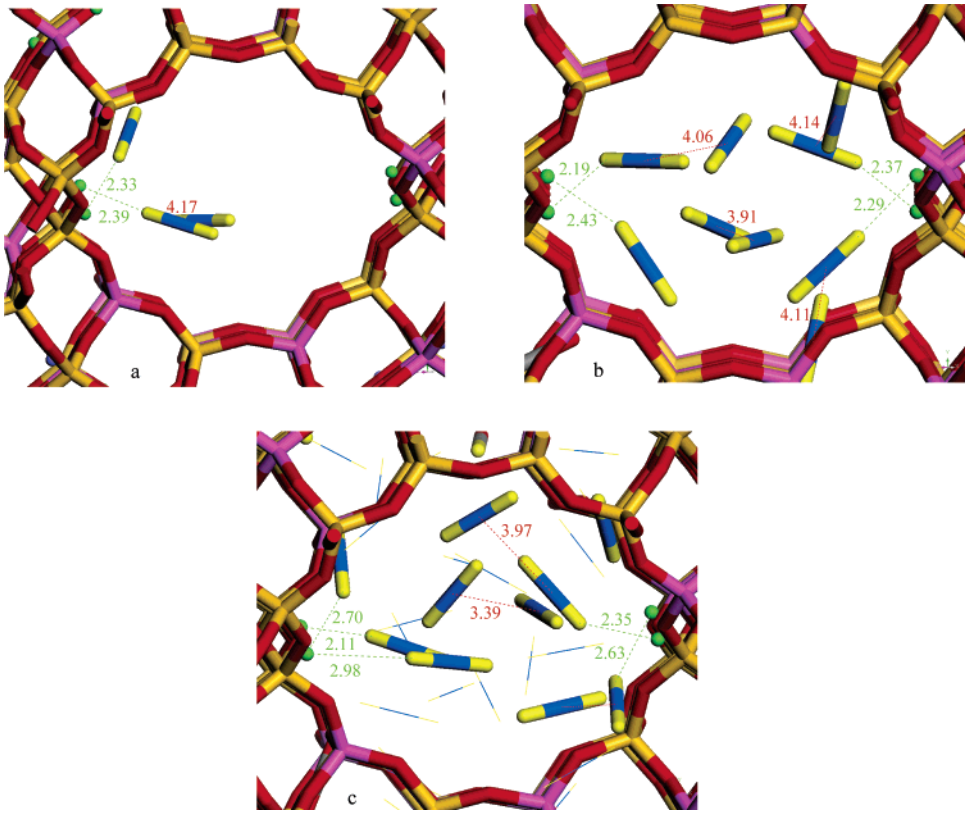

Figure 7. Typical arrangements of the CO_2 molecules in NaY for low ((a) 0.1 bar), intermediate ((b) 1 bar), and high ((c) 25 bar) coverage. Na^+ located in site II is represented in green, and the typical distances $Na-O_z$ and O_z-O are reported in angstroms.

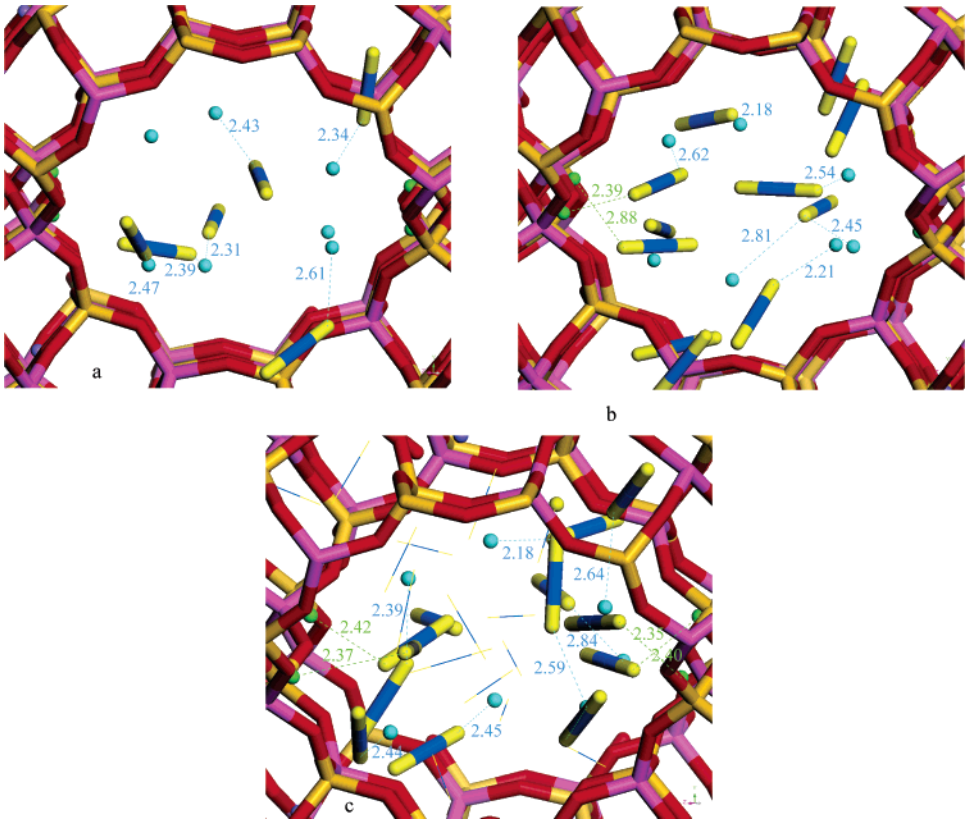

Figure 8. Typical arrangements of the CO_2 molecules in NaLSX for low ((a) 0.1 bar), intermediate ((b) 1 bar), and high ((c) 20 bar) loading. Na^+ located in sites II and III′ are represented in green and light blue, respectively, and the typical distances $Na-O_z$ (Å) are reported.

to the solvation process whereas the energy part of the CO_2/CO_2 interactions increases. The combination of these two contributions leads to the relative constant value of the differential enthalpy of adsorption when the loading increases.

The differential enthalpy of adsorption measured experimentally for NaLSX (Figure 4) sharply decreases as the loading increases, the simulated trend corresponds to a smoother, continuous decrease. Similar enthalpy profiles have been

previously reported[28,29,31,57,58] with differential enthalpies of adsorption at low coverage ranging from 45 to 49 kJ mol^{-1} in accordance with the extrapolated values of 45.3 and 44.2 kJ mol^{-1} obtained from our experiments and simulations, respectively. Furthermore, our simulation emphasized the existence of two adsorption sites located close to Na^+ in sites II and III′. As depicted in Figure 8a, the carbon dioxide molecules preferentially interact with extraframework cations in site III′ at the initial stage of adsorption. For intermediate and high loading, when the surrounding environment of Na^+ in site III′ is fully occupied, the adsorbates occupy sites of lower energy by interacting with the Na^+ in site II (parts b and c of Figure 8). The existence in NaLSX zeolite of two types of CO_2 adsorption sites has also been inferred from diffuse reflectance IR Fourier transform spectroscopy.[59] Indeed, CO_2 probes NaLSX as a heterogeneous energetic surface by interacting preferentially with Na^+ in site III′ and further occupying less favorable sites close to Na^+ in site II, which gives rise to a decrease of the CO_2/adsorbent interaction energy when the loading increases. This contribution, combined with an increase of the CO_2/CO_2 interaction energy, leads to a decrease of the differential enthalpy of adsorption as coverage increases. Furthermore, a similar behavior is observed for the orientation of the CO_2 molecules with respect to Na^+ as was already mentioned in the case of NaY.

5. Conclusions

The force field derived from ab initio calculations for representing the interactions between carbon dioxide and zeolite adsorbent was revealed to be very well transferable as it allowed accurate reproduction of the microcalorimetry data in three different faujasite forms, DAY, NaY, and NaLSX, via GCMC simulations. It is the first time that a force field developed for carbon dioxide has given such good results in zeolite systems across a wide range of pressure. This modeling approach can be envisaged as a predictive tool in order to easily evaluate the performance of different types of zeolite materials with respect to CO_2 and thus to define the specific characteristics of the adsorbent especially adapted for the CO_2 storage and separation, which is of great environmental and economical interest. Furthermore, we proposed a microscopic mechanism for CO_2 adsorption for each system investigated, which is consistent with the evolution of the differential enthalpy of adsorption as a function of the coverage. It clearly states that CO_2 probes DAY, NaY, and NaLSX as different types of energetic surfaces. We have thus shown that microcalorimetry combined with atomistic simulation is a powerful tool able to deeper understand the interactions between the adsorbent surface and the adsorbate molecules.

Acknowledgment. This work was supported by EU fundings via FP6-Marie Curie Research Training Network "INDENS" (MRTN-CT-2004-005503).

References and Notes

(1) Kikuchi, R. *Energy Environ.* **2003**, *14* (4), 383.
(2) Kikkinides, E. S.; Yang, R. T.; Cho., S. H. *Ind. Eng. Chem. Res*. **1993**, *32*, 2714.
(3) Epstein, P. R. Inside the Greenhouse: the impact of CO_2 and climate change on public health in the inner city, center for health and the global environment, April 29, 2004, Harvard Medical School.
(4) Bargigli, S.; Raugei, M.; Ulgiati, S. *Energy* **2004**, *29*, 2145.
(5) Singh, D.; Croiset, E; Douglas, P. L.; Douglas, M. A. *Energy Convers. Manage*. **2003**, *44* (19), 3073.
(6) Ruthven, D. M.; Shamasuzzaman, F.; Knaebel, K. S. *Pressure Swing Adsorption*; VCH Publishers: New York, 1994.
(7) Meier, W. M.; Olson, D. H. *Atlas of zeolite structures*, Structure Commission of the International Zeolite Association; Elsevier: Amsterdam, The Netherlands, 1978. http://www.iza-structure.org.
(8) Siriwardane, R. V.; Shen, M. S.; Fisher, E. P.; Poston, J. A. *Energy Fuels* **2001**, *15*, 279.
(9) Goj, A.; Sholl, D. S.; Akten, E. D.; Kohen, D. *J. Phys. Chem. B* **2002**, *106*, 8367.
(10) Maurin, G.; Llewellyn, P. L.; Poyet, T.; Kuchta, B. *J. Phys. Chem. B.* **2005**, *109*, 125.
(11) Savitz, S.; Myers, A. L.; Gorte, R. J. *Microporous Mesoporous Mater*. **2000**, *37*, 33.
(12) Jacobs, P. A.; Van Santen, R. A. *Studies in Surface Science and Catalysis*; Elsevier: Amsterdam, The Netherlands, 1989; Vol. 49.
(13) Kyam, K.; Shibata, T.; Watanabe, F.; Matsuda, H.; Hasatani, M. *Energy Convers. Manage.* **1997**, *38*, 10−13, 1025.
(14) Harlick, P. J. E.; Handan Tezel, F. *Microporous Mesoporous Mater*. **2004**, *76*, 71.
(15) Mizukami, K.; Takaba, H.; Konayashi, Y.; Oumi, Y.; Belosludov, R. V.; Takami, S.; Kubo, M.; Miyamoto, A. *J. Membr. Sci*. **2001**, *188*, 21.
(16) Bonhomme, F.; Welk, M. E.; Nenoff, T. N. *Microporous Mesoporous Mater*. **2003**, *66*, 181.
(17) Gheno, S. M.; Damyanova, S.; Riguetto, B. A.; Marques, C. M. P.; Leite, C. A. P.; Bueno, J. M. C. *J. Mol. Catal. A: Chem.* **2003**, *198*, 263.
(18) Liu, B. S.; Gao, L. Z.; Au, C. T. *Appl. Catal., A* **2002**, *235*, 193.
(19) Barbieri, G.; Marigliano, G.; Golemme, G.; Drioli, E. *Chem. Eng. J.* **2002**, *85*, 53.
(20) Levy, M.; Levitan, R.; Rosin, H.; Rubin, R. *Sol. Energy* **1993**, *50*, 179.
(21) Akten, E. D.; Siriwardane, R.; Sholl, D. S. *Energy Fuels* **2003**, *17*, 977.
(22) Hirotani, A.; Mizukami, K.; Miura, R.; Takaba, H.; Miya, T.; Fahmi, A.; Stirling, A.; Kubo, M.; Miyamoto, A. *Appl. Surf. Sci.* **1997**, *120*, 81.
(23) Gao, W.; Butler, D.; Tomasko, D. L. *Langmuir* **2004**, *20*, 8083.
(24) MacDonald, J. A. F.; Quinn, D. F. *Fuel* **1998**, *77*, 61.
(25) Lee, J. S.; Kim, J. H.; Kim, J. T.; Suh, J. K.; Lee, J. M.; Lee, C. H. *J. Chem. Eng. Data* **2002**, *47*, 1237.
(26) Choudhary, V. R.; Mayadevi, S.; Pal Singh, A. *J. Chem. Soc., Faraday Trans.* **1995**, *91*, 2935.
(27) Choudhary, V. R.; Mayadevi, S. *Zeolites* **1996**, *17*, 501.
(28) Barrer, R. M.; Gibbons, R. M. *Trans. Faraday Soc*. ***1965***, *61*, 948.
(29) Dunne, J. A.; Mariwala, R.; Rao, M.; Sircar, S.; Gorte, J.; Myers, A. L. *Langmuir* **1996**, *12*, 5888.
(30) Dunne, J. A.; Rao, M.; Sircar, S.; Gorte, R. J.; Myers, A. L. *Langmuir* **1996**, *12*, 5896.
(31) Khvoshchev, S. S.; Zverev, A. V. *J. Colloid Interface Sci.* **1991**, *144*, 571.
(32) Rouquerol, F.; Rouquerol, J.; Sing, K. *Adsorption by powders and porous solids*; Academic Press: London, 1999.
(33) Llewellyn, P. L.; Maurin, G. *C.R. Chim.* **2005**, *8*, 253.
(34) Llewellyn, P. L.; Coulomb, J. P.; Grillet, Y.; Patarin, J.; Lauter, H.; Reichert, H.; Rouquerol, J. *Langmuir* **1993**, *9*, 1846.
(35) Fuchs, A. H.; Cheetham, A. K. *J. Phys. Chem. B* **2001**, *105*, 7375.
(36) Loisruangsin, A.; Fritzsche, S.; Hannongbua, S. *Chem. Phys. Lett*. **2004**, *390* (4−6), 485.
(37) Nakazaki, Y.; Tanaka, Y.; Goto, N.; Inui, T. *Catal. Today* **1995**, *23*, 3391.
(38) Makrodimitris, K.; Papadopoulos, G. K.; Theodorou, D. N. *J. Phys. Chem. B* **2001**, *105*, 777.
(39) Mortier, W. J. *Compilation of Extraframework Sites in Zeolites*; Butterworth: Guildford, U.K., 1982.
(40) Maurin, G.; Llewellyn, P. L.; Poyet, Th.; Kuchta, B. *Microporous Mesoporous Mater*. **2005**, *79*, 53.
(41) Rouquerol, J. *Thermochim. Acta* **1989**, *144*, 209.
(42) Redlich, O.; Kwong, J. N. S. *Chem. Rev*. **1949**, *44*, 233.
(43) Moret, S.; Poyet, T.; Rouquerol, F.; Rouquerol, J.; Llewellyn, P. L. *Stud. Surf. Sci. Catal*. **2002**, *144*, 723.
(44) Fitch, A. N.; Jobic, H.; Renouprez, A. *J. Phys. Chem. B* **1986**, *90* 1311.
(45) Lowenstein, W. *Am. Mineral*. **1954**, *39*, 92.
(46) Zhu, L.; Seff, K. *J. Phys. Chem. B* **1999**, *103*, 9512.
(47) Bell, R. G.; et al. Manuscript in preparation.
(48) Demontis, P.; Suffriti, G. B. *Chem. Rev.* **1997**, *97*, 2845.
(49) Nicholson, D.; Parsonage, N. G. *Computer simulation and the statistical mechanics of adsorption*; Academic Press: London, 1982.
(50) Mellot-Draznieks, C.; Rodriguez-Carjaval, J.; Cox, D. E.; Cheetham, A. K. *Phys. Chem. Chem. Phys*. **2003**, *5*(9), 1882.
(51) Rees, L. V. C.; Brückner, P.; Hampson, J. *Gas Sep. Purif.* **1991**, *5*, 67.
(52) Maurin, G.; Llewellyn, P. L.; Bell, R. G. *Stud. Surf. Sci. Catal*. In press.
(53) Burevski, D.; Pilchowski, K.; Bergk, K. H. *Croat. Chem. Acta* **1991**, *64*, 2, 199.

(54) Concepcion-Heydorn, P.; Jia, C.; Herein, D.; Pfänder, N.; Karge, H. G.; Jentoft, F. C. *J. Mol. Catal. A: Chem.* **2000**, *162*, 227.
(55) Bonelli, B.; Civalleri, B.; Fubini, B.; Ugliengo, P., Otero Arean, C.; Garonne, E. *J. Phys. Chem. B* **2000**, *104*, 10978.
(56) Garrone, E.; Bonelli, B.; Lamberti, C.; Civallen, B.; Rocchia, M.; Roy, P.; Otero Arean, C. *J. Chem. Phys*. **2002**, *117*, 22, 10274.
(57) Khelifa, A.; Derriche, Z.; Bengueddach, A. *Microporous Mesoporous Mater*. **1999**, *32*, 199.
(58) Shen, D.; Bülow, M. *Microporous Mesoporous Mater*. **1998**, *22*, 237.
(59) Kazansky, V. B.; Borovkov, V. Y.; Serykh, A. I.; Bülow, M. *Phys. Chem. Chem. Phys*. **1999**, *1*, 3701.